Synchronization transitions in globally coupled rotors in the presence of noise and inertia: Exact results

2014 EPL 106 40003

(http://iopscience.iop.org/0295-5075/106/4/40003)

A Letters Journal Exploring the Frontiers of Physics

May 2014

EPL, **106** (2014) 40003 www.epljournal.org
doi: 10.1209/0295-5075/106/40003

Synchronization transitions in globally coupled rotors in the presence of noise and inertia: Exact results

Maxim Komarov[1,2], Shamik Gupta[3] and Arkady Pikovsky[1,2]

[1] *Department of Physics and Astronomy, Potsdam University - Karl-Liebknecht-Str 24, D-14476, Potsdam, Germany*
[2] *Department of Control Theory, Nizhni Novgorod University - Gagarin Av. 23, 606950, Nizhni Novgorod, Russia*
[3] *Laboratoire de Physique Théorique et Modèles Statistiques (CNRS UMR 8626), Université Paris-Sud - Orsay, France*

received 20 February 2014; accepted in final form 28 April 2014
published online 22 May 2014

PACS 05.45.Xt – Synchronization; coupled oscillators
PACS 05.70.Fh – Phase transitions: general studies
PACS 05.70.Ln – Nonequilibrium and irreversible thermodynamics

Abstract – We study a generic model of globally coupled rotors that includes the effects of noise, phase shift in the coupling, and distributions of moments of inertia and natural frequencies of oscillation. As particular cases, the setup includes previously studied Sakaguchi-Kuramoto, Hamiltonian and Brownian mean-field, and Tanaka-Lichtenberg-Oishi and Acebrón-Bonilla-Spigler models. We derive an exact solution of the self-consistent equations for the order parameter in the stationary state, valid for arbitrary parameters in the dynamics, and demonstrate nontrivial phase transitions to synchrony that include reentrant synchronous regimes.

Introduction. – Synchronization in a large population of coupled oscillators of distributed natural frequencies is a remarkable example of a nonequilibrium phase transition. The paradigmatic minimal model to study synchronization is the one due to Kuramoto, introduced almost 40 years ago [1], based on an earlier work by Winfree [2]. Over the years, many details of the Kuramoto model [3,4], and applications to various physical [5], chemical [6], biological [7], engineering [8], and even social problems [9] have been addressed in the literature.

The Kuramoto model comprises oscillators that are described by their phases, have natural frequencies given by a common distribution, and are subject to a global mean-field coupling. The phases follow a first-order dynamics in time. In the simplest setup of a purely sinusoidal coupling without a phase shift, and for a unimodal distribution of frequencies, the model exhibits a continuous (second-order) transition from an unsynchronized to a synchronized phase as the coupling constant exceeds a critical threshold. The phase transition appears as a Hopf bifurcation for the complex order parameter.

The dynamics of the Kuramoto model is intrinsically dissipative. When all the oscillators have the same frequency, the analogue of the model in the realm of energy-conserving Hamiltonian dynamics is the so-called Hamiltonian mean-field model (HMF) [10,11]. In this case, the dynamical equations are the Hamilton equations: the oscillator phases follow a second-order dynamics in time, *i.e.*, the system constituents are in fact not oscillators, but rotors. In order to include the effects of interaction with an external heat bath, it is natural to consider the HMF evolution in the presence of a Gaussian thermostat. In the resulting Brownian mean-field (BMF) model, the dynamical equations are damped and noise-driven [12,13]. Both the HMF and the BMF model have an equilibrium stationary state that exhibits a continuous phase transition between a synchronized phase at low values of energy/temperature and an unsynchronized phase at high values. On considering the BMF model with nonidentical oscillator frequencies, the dynamics violates the detailed balance leading to a nonequilibrium stationary state (NESS) [14]. In the overdamped limit, the dynamics reduces to that of the noisy Kuramoto model involving Kuramoto dynamics in the presence of Gaussian noise, which was introduced to model stochastic fluctuations of the natural frequencies in time [15]. The resulting phase diagram is complex, with both continuous and first-order transitions [14].

In this work, we study a generic model of globally coupled rotors, in which two types of deviations from equilibrium are included: i) a distribution of torques acting on the rotors, similar to the distribution of frequencies in the Kuramoto model, and ii) a phase shift in the coupling, that makes the latter non-Hamiltonian. We consider the rotors to have quite generally different moments of inertia given by a common distribution [16]. Our setup includes as special cases previously studied Sakaguchi-Kuramoto [17], Hamiltonian and Brownian mean-field, Tanaka-Lichtenberg-Oishi [18], and Acebrón-Bonilla-Spigler [19,20] models.

The basic roadblock in studying out-of-equilibrium dynamics, in particular, in characterizing the resulting long-time NESSs is the lack of a framework that allows to treat such states on a general footing, akin to the one for equilibrium steady states *à la* Gibbs-Boltzmann. Even for simple nonequilibrium models, obtaining the steady-state distribution has been a *tour de force* [21], while in many cases, the analytical characterization of the steady state has so far been elusive, thereby requiring one to resort to numerical simulations and approximation methods [22].

In this backdrop, it is remarkable that for our system of study, we are able to characterize exactly the NESS under quite general conditions. In the thermodynamic limit $N \to \infty$, we study the system by analyzing the Kramers equation for the evolution of the single-rotor phase space distribution. Using the combination of an analytical approach to solve the Kramers equation in the steady state [23] and a novel self-consistency approach [24,25], we formulate an exact equation for the complex order parameter as a function of the relevant parameters of the system, for arbitrary distributions of torques and moments of inertia. As applications of our approach, we provide for suitable and representative choices of the distribution function several nontrivial illustrations of transitions to synchrony, including in some cases interesting reentrant synchronous regimes.

Basic model. – The equations of motion for the i-th rotor read

$$m_i\ddot{\phi}_i + \gamma\dot{\phi}_i = \gamma\nu_i + \mathcal{K}R\sin(\psi - \phi_i - \beta) + \sqrt{\gamma T}\ \eta_i, \quad (1)$$

where dots denote differentiation with respect to time τ. Here, ϕ_i is the angle of the i-th rotor, γ is the friction constant, $\mathcal{K}$ is the coupling constant, β is the phase shift parameter, T is the temperature in units of the Boltzmann constant, while R and ψ constitute the complex order parameter of the problem: $R(\tau)e^{i\psi(\tau)} \equiv \sum_{j=1}^{N} e^{i\phi_j(\tau)}/N$. Note that R is the magnitude while ψ is the phase of the mean field acting on the rotors. In the dynamics (1), the term $\gamma\nu_i$ is the external torque acting on the i-th rotor. The parameters of the rotors, namely, their frequencies ν_i's and the moments of inertia m_i's, are quenched random variables sampled from a common distribution $g(\nu, m)$. The noise $\eta_i(\tau)$ is Gaussian and white, with $\langle\eta_i(\tau)\rangle = 0$, $\langle\eta_i(\tau)\eta_j(\tau')\rangle = 2\delta_{ij}\delta(\tau-\tau')$. The fluctuation-dissipation theorem implies the factor $\sqrt{\gamma T}$ in the noise term in eq. (1). To reduce the number of relevant parameters, we introduce dimensionless variables $t \equiv \tau T/\gamma$, $M_i \equiv m_i T/\gamma^2$, $K = \mathcal{K}/T$, $\omega_i = \gamma\nu_i/T$, in terms of which eq. (1) becomes (with dots now denoting derivative with respect to t)

$$M_i\ddot{\phi}_i + \dot{\phi}_i = \omega_i + KR\sin(\psi - \phi_i - \beta) + \eta_i, \quad (2)$$

involving two dimensionless parameters K and β; here, $\eta_i(t)$ is a Gaussian white noise with $\langle\eta_i(t)\rangle = 0, \langle\eta_i(t)\eta_j(t')\rangle = 2\delta_{ij}\delta(t-t')$. Additional parameters describe the distribution $G(\omega, M)$ of dimensionless natural frequencies and moments of inertia.

For the dynamics (2), we seek for NESS with nonzero, uniformly rotating mean field, which generally has a frequency Ω different from the mean frequency of the natural frequency distribution. Transforming to the reference frame rotating with frequency Ω, as $\psi \equiv \Omega t + \psi_0, \phi_i \equiv \theta_i + \psi - \beta$, where ψ_0 is a constant, eq. (2) reads

$$M_i\ddot{\theta}_i + \dot{\theta}_i = \omega_i - \Omega - KR\sin\theta_i + \eta_i(t). \quad (3)$$

In terms of the new variables θ_i, the equations of motion no longer contain the phase shift β in the coupling function; however, now, the unknown frequency Ω appears as a parameter on the right-hand side of eq. (3). The new complex order parameter $\tilde{R}(t)e^{i\tilde{\psi}(t)} \equiv \sum_{j=1}^{N} e^{i\theta_j(t)}$ can be expressed using the old one as $\tilde{R}(t)e^{i\tilde{\psi}(t)} = R(t)e^{i\beta}$. This implies that the magnitude of the order parameter is conserved in this transformation, $\tilde{R}(t) = R(t)$. Moreover, the argument of the new order parameter determines the phase shift in eq. (2), $\beta = \tilde{\psi}$. From now on, we focus on analyzing the dynamics (3).

At this point, it is instructive to link model (3) to previously studied setups. Consider the model without the phase shift parameter, *i.e.*, $\beta = 0$, leading to a symmetric coupling function. Let us next specialize to the case $G(\omega, M) = \delta(M - M_0)g(\omega)$. When the frequency distribution $g(\omega)$ is a delta function, $g(\omega) = \delta(\omega - \omega_0)$, so that $\omega_i = \Omega = \omega_0$, eq. (3) describes the BMF model. This model has an equilibrium stationary state in which the system exhibits a continuous phase transition between a synchronized ($R \neq 0$) and an unsynchronized ($R = 0$) phase at the critical coupling $K_c = 2$ [12,13]. When $g(\omega)$ is not a delta function, the dynamics (3) drives the system to a NESS [14]. In particular, for $M_0 = 0$, the dynamics corresponds to the $\beta = 0$ case of the Sakaguchi-Kuramoto model with the inclusion of noise. Then, taking $g(\omega)$ to be unimodal with width D, the model shows a continuous synchronization phase transition across $K_c(D)$ described in ref. [15]. In our normalization, the intensity of noise is set to one, thus the noiseless situation corresponds to the limit $K, D \to \infty$. This noiseless dynamics defines the Tanaka-Lichtenberg-Oishi model [18]. In ref. [20], for model (3) with $G(\omega, M) = \delta(M - M_0)g(\omega)$ and $\beta = 0$ (the Acebrón-Bonilla-Spigler model), a linear stability analysis and an approximate treatment of the transition to synchrony have been performed. In both these works, a first-order transition to synchrony was revealed.

Thermodynamic limit: the Kramers equation and its self-consistent stationary solution. – We now consider the dynamics (3) in the thermodynamic limit $N \to \infty$. In this limit, the dynamics is characterized by the single-rotor conditional distribution

$\rho(\theta, v, t|\omega - \Omega, M)$, which gives at time t and for the given set of parameters (ω, M) the fraction of rotors with angle θ and angular velocity $v = \dot{\theta}$. The distribution is 2π-periodic in θ, and obeys the normalization $\int_0^{2\pi} \mathrm{d}\theta \int_{-\infty}^{\infty} \mathrm{d}v\ \rho(\theta, v, t|\omega - \Omega, M) = 1$, while evolving toward a stationary distribution following the Kramers (Fokker-Planck) equation [14]

$$\frac{\partial \rho}{\partial t} = -v\frac{\partial \rho}{\partial \theta} + \frac{\partial}{\partial v}\left[\frac{1}{M}\Big(v - \omega + \Omega + A\sin\theta\Big)\rho\right] + \frac{1}{M^2}\frac{\partial^2 \rho}{\partial v^2}, \tag{4}$$

where we have defined $A \equiv KR$. In the steady state, R is time-independent, with

$$Re^{i\beta} = \int \mathrm{d}W G(\omega + \Omega, M)e^{i\theta}\rho(\theta, v|\omega, M) \equiv F(\Omega, A), \tag{5}$$

where $\mathrm{d}W = \mathrm{d}\theta\mathrm{d}v\mathrm{d}\omega\mathrm{d}M$. The stationary distribution $\rho(\theta, v|\omega - \Omega, M)$ depends on the unknown quantities A and Ω, which we, from now on, consider as given parameters. The representation (5) gives the solution of the problem in a parametric form: the order parameter R and the coupling parameters, K, β, are expressed as explicit functions of A and Ω, as

$$R = |F(\Omega, A)|, \quad K = \frac{A}{|F(\Omega, A)|}, \quad \beta = \mathrm{arg}F(\Omega, A). \tag{6}$$

By varying Ω and A, while keeping the parameters of the distribution $G(\omega, M)$ fixed, we find the order parameter R as a function of K and β (cf. [24,25]).

The stationary solution of the Kramers equation (4) is described in [23]. One looks for a solution in the form of a double expansion in Fourier modes in θ and Hermite functions in v as

$$\rho(\theta, v|\omega - \Omega, M) = (2\pi)^{-1/2}\Phi_0(v)\sum_{n=0}^{\infty}\sum_{k=-\infty}^{\infty} a_{n,k}(\omega - \Omega, M)\Phi_n(v)e^{ik\theta}, \tag{7}$$

where $\Phi_n(v)$ are the Hermite functions: $\Phi_n(v) = \sqrt{\alpha}/(\sqrt{2^n n!\sqrt{\pi}})\exp[-v^2\alpha^2/2]H_n(\alpha v)$; $\alpha = \sqrt{M/2}$. Note that ρ being real, it follows that $a^*_{n,k} = a_{n,-k}$, where $*$ denotes complex conjugation. By inserting the expansion (7) into the Kramers equation in the stationary state, one obtains a linear system of equations for coefficients $a_{n,k}$, which can be solved using the matrix continued fraction method [23]. Substituting expansion (7) into eq. (5), we find that

$$F(\Omega, A) = \sqrt{2\pi}\int \mathrm{d}\omega\mathrm{d}M G(\omega, M)a^*_{0,1}(\omega - \Omega, M). \tag{8}$$

According to the matrix continued fraction method [23], the coefficient $a_{0,1}$ can be found from the matrix $\mathbf{H}$, as

$$a_{0,1}(\nu, M) = H^{1,0}(\nu, M)/\left(\sqrt{2\pi}H^{0,0}(\nu, M)\right), \tag{9}$$

where $\mathbf{H}(\nu, M)$ is given by the following recurrent formula:

$$\mathbf{H} = -\frac{1}{\sqrt{M}}\widetilde{\mathbf{D}}^{-1}\Bigg(\mathbf{I} - M\mathbf{D}\Bigg[\mathbf{I} - \frac{M}{2}\mathbf{D}(\mathbf{I} - \frac{M}{3}\{\mathbf{D}[\mathbf{I} - \ldots]\}^{-1}\widetilde{\mathbf{D}})^{-1}\widetilde{\mathbf{D}}\Bigg]^{-1}\widetilde{\mathbf{D}}\Bigg), \tag{10}$$

with the matrix $\mathbf{D} = ik\delta_{n,k}$, while the matrix $\widetilde{\mathbf{D}}$ is

$$\widetilde{D}^{n,k} \equiv \left(\Big(ik - \nu\Big)\delta_{n,k} - i\Big(\delta_{n,k+1} - \delta_{n,k-1}\Big)\frac{A}{2}\right). \tag{11}$$

The construction of the exact solution for the order parameter consists now of the following steps. i) The recurrence formula (10) yields the matrix $\mathbf{H}$, and thus, according to relation (9), the value of $a_{0,1}$ for any set of ω, Ω, A, M. ii) The substitution of these values into integral (8) yields the complex function $F(\Omega, A)$. iii) With the help of eq. (6), we get the order parameter R and the parameters K, β as functions of Ω, A, which constitutes the analytic solution in a parametric form. In order to evaluate this solution numerically, several approximations are needed. In step i), we do not calculate an infinite matrix, but instead truncate the Fourier and the Hermite series such that $n = 0, \ldots, \tilde{N}$ and $k = -\tilde{K}, \ldots, \tilde{K}$. After that, fixing a certain discretization grid on the plane (ν, M), we calculate finite-dimensional matrices $\mathbf{D}$ and $\widetilde{\mathbf{D}}$. The latter allows us to calculate the finite matrix $\mathbf{H}(\nu, M)$ with desired accuracy, using a finite number of recurrence steps in (10). In step ii), we perform the integration using a summation on the grid. The basic parameters determining numerical accuracy are the truncation numbers $\tilde{N}$, $\tilde{K}$ and the parameters of the grid (ν, M); they were determined in such a way as not to change the final result beyond a given accuracy. In the following sections, we present several applications of our approach to compute the steady state R for representative choices of the frequency and moment of inertia distribution and parameters of the dynamics, and highlight possible synchronization transitions.

Phase transitions in the case of symmetric coupling function (*i.e.*, $\beta = 0$). – Here, we consider the symmetric, Hamiltonian coupling, *i.e.*, with the phase shift $\beta = 0$. As one can see from (6), the function F, given by eqs. (5) and (8), should be real. Let us choose for each moment of inertia M the distribution $G(\omega, M)$ to be symmetric about its mean Ω_0: $G(\omega - \Omega_0, M) = G(\Omega_0 - \omega, M)$. Then, using eq. (8) and the fact that F is real, one arrives at the consistent conclusions that $\Omega = \Omega_0$ and $a_{0,1}(\nu, M) = a^*_{0,1}(-\nu, M)$. (For a general asymmetric distribution, like eq. (15) below, to be consistent with $\beta = 0$, one has to vary Ω to find the value at which $\mathrm{arg}F(\Omega, A) = 0$). As the simplest example of such a situation, we consider the case of equal moments of inertia, and a Gaussian distribution with mean zero and width D for the frequencies $G(\omega, M) = \delta(M - M_0)g(\omega)$, with $g(\omega) = 1/(\sqrt{2\pi D^2})\exp[-\omega^2/(2D^2)]$. In fig. 1, we report the phase diagram in the three-dimensional space of

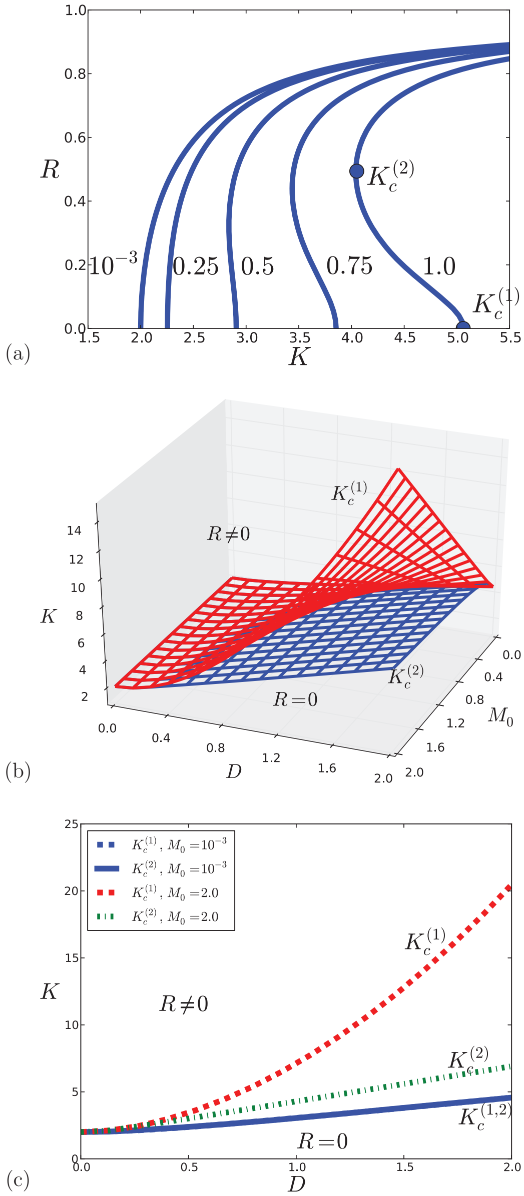

Fig. 1: (Colour on-line) For $G(\omega, M) = \delta(M - M_0)g(\omega)$, with $g(\omega)$ being a Gaussian with zero mean and width D, (a) shows the order parameter R as a function of K for $M_0 = 1$ and for various values of D marked in the figure. For sufficiently large D, the synchronized phase arises as a first-order phase transition from the unsynchronized phase, with two characteristic thresholds, $K_c^{(1)}$ and $K_c^{(2)}$. (b) Surfaces $K_c^{(1)}$ and $K_c^{(2)}$ in the three-dimensional M_0-K-D space. (c) Sections of the surfaces $K_c^{(1)}$ and $K_c^{(2)}$ in (b) for different values of M_0.

parameters M_0, K, D, stressing on the synchronized and unsynchronized states. The previously known limits are 1) for $M_0 = 0$, when one has the line $K_c(D)$ for the continuous transition given by $K_c(D) = 2[\int_{-\infty}^{\infty} \mathrm{d}\omega\, g(\omega)/(\omega^2 + 1)]^{-1}$ [15], 2) for $D = 0$, when one has the continuous transition point of the BMF model given by $K_c \equiv K_c(0) = 2$, independent of M_0 [12,13]. For $M_0, D \neq 0$, one expects a first-order phase synchronization transition characterized by two thresholds $K_c^{(1)}$ and $K_c^{(2)}$, where the former is the stability threshold of the unsynchronized phase, while $K_c^{(2)}$ is the point at which two branches of synchronized solutions arise [14]. These observations are borne out by our numerical results depicted in fig. 1. Panel (a) shows R as a function of K at a fixed M_0 and for different values of D: one may observe that at large D, the synchronized phase arises as a first-order transition from the unsynchronized phase.

Nonuniversal phase transitions in the case of phase shift in coupling. – In this section, we illustrate several examples of nontrivial and nonuniversal phase transitions to synchrony in the case of nonzero β, by choosing $G(\omega, M) = \delta(M - M_0)g(\omega)$, where we choose a nontrivial symmetric $g(\omega)$ that is known to yield a nonuniversal transition in the Sakaguchi-Kuramoto model [25]:

$$g(\omega) = \begin{cases} p\dfrac{D-\omega}{D^2} + (1-p)\dfrac{qD-\omega}{q^2D^2}; & \omega \leq qD, \\ \dfrac{D-\omega}{D^2}; & \omega > qD. \end{cases} \tag{12}$$

The results are shown in fig. 2. Panel (a) shows two examples of a reentrant synchronization transition: with increase of the coupling constant, synchrony first appears but disappears at larger coupling, beyond which there is a second threshold. Figure 2(b) shows that this behavior depends on the value of M_0 in a nontrivial way: while the reentrance is observed for small and large M_0, it is absent for intermediate values. Finally, in fig. 2(c), we illustrate how the reentrant behavior depends on noise. As the noise intensity is set to one in our scheme of normalization, we simultaneously varied parameters M_0 and D according to $M_0 = \widetilde{M}_0\sigma$, $D = D_0/\sigma$, with $\widetilde{M}_0 = 0.1$, $D_0 = 5$. The resulting path in the (M_0, D)-plane corresponds effectively to the variation of the noise intensity, with $\sigma \sim T$. One can see that with increase of the noise, the area of nontrivial transitions marked in grey shrinks and disappears. The inset illustrates how the region of the reentrance is determined from the solution. It shows the values of $\beta(\Omega)$ for vanishing mean field $A = 0^+$, *i.e.* at the transition points. At $\sigma = 0.025$ (dashed curve in (c) (inset)), there is a nonmonotonic dependence of β on Ω. Thus, in the region between the local extrema, there are three values of Ω that give the same value of β. These three values correspond to the different branches in each of the $R(K)$ plots in fig. 2(a) at which the value of the order parameter vanishes (*i.e.* the values of K at which synchrony appears, disappears, and appears again). At relatively strong noise ($\sigma = 0.1$, solid curve in (c) (inset)), there is a monotonic dependence of β on Ω, with only one transition to synchrony.

Phase transitions in populations with distribution of moments of inertia. – In this section, we present several examples of phase transitions by choosing nontrivial distributions for both moments of inertia

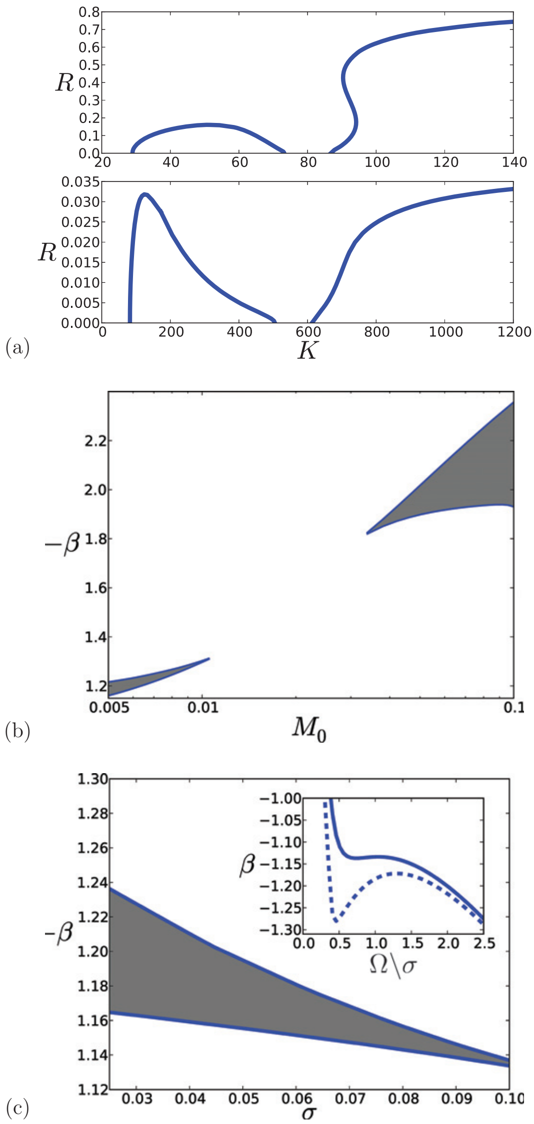

Fig. 2: (Colour on-line) (a) Examples of nonuniversal transitions for $G(\omega, M) = \delta(M - M_0)g(\omega)$, with $g(\omega)$ given by eq. (12). Parameters are $M_0 = 5 \times 10^{-3}$, $\beta = -1.164$ (upper panel), and $M_0 = 0.06$, $\beta = -1.95$ (lower panel). In both cases, $p = 0.6$, $D = 100$, $q = 0.08$. (b) Regions in the (M_0, β)-plane with complex nontrivial transitions marked in grey, for the same parameters of the frequency distribution as in panel (a). (c) Dependence of the region of reentrance (gray regions in (b)) on the effective noise intensity (see main text); the increase of σ corresponds to the linear increase of the noise intensity.

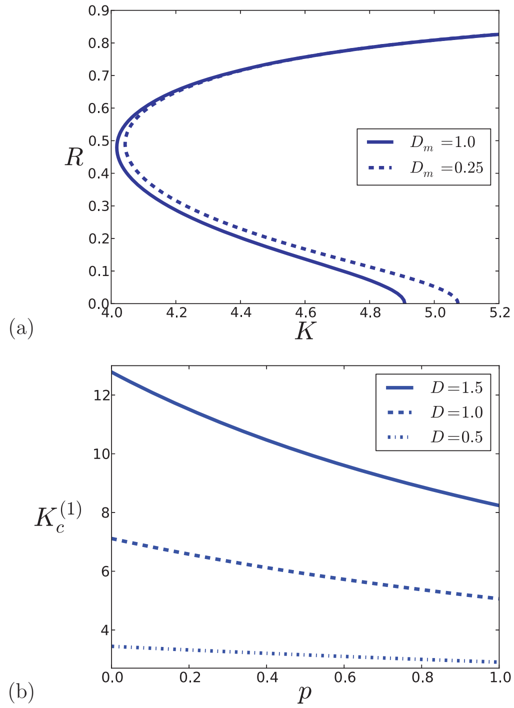

Fig. 3: (Colour on-line) (a) $R(K)$ for the distribution (13) with two different values of D_m but with the same mean moment of inertia $M_0 = 1.01$. (b) For the distribution (14), the figure shows the dependence of $K_c^{(1)}$ on the parameter p for different values of D (width of the frequency distribution $g(\omega)$).

and frequencies. In the first example, we used independent distributions of moments of inertia and frequencies: $G(M, \omega) = g(\omega)f(M)$, with

$$f(M) = \begin{cases} \dfrac{1}{C}\left[1 - \dfrac{(M - M_0)^2}{D_m^2}\right], & |M - M_0| \le D_m, \\ 0, & |M - M_0| > D_m. \end{cases} \qquad (13)$$

Thus, the moments of inertia are distributed according to a simple parabolic shape with characteristic width D_m (C is the normalization constant), while for frequencies, we use a Gaussian distribution with mean zero and width D. In fig. 3(a), dependences of the order parameter on the coupling are presented for two distributions for different D_m's, but with the same mean moment of inertia M_0. One can see that the more diverse is the population, the easier it is to synchronize. To reveal the underlying mechanism, we calculated the synchronization threshold $K_c^{(1)}$ in a more simple setup of rotors having just two different moments of inertia, *i.e.*, the distribution is a sum of two delta functions:

$$f(M) = p\delta(M - M_0) + (1 - p)\delta(M - M_1), \qquad (14)$$

where we assume that $M_0 < M_1$. By increasing the parameter p from 0 to 1, we increase the fraction of light particles in the population. Figure 3(b) shows that the critical coupling $K_c^{(1)}$ decreases with p: One can see that the addition of light particles always leads to a decrease of $K_c^{(1)}$, implying ease of the population to synchronize with more lighter particles; this is consistent with the result in fig. 3(a).

In the second example, we illustrate a situation where the symmetry of the frequency distribution is broken in a nontrivial way, through a correlation with the moments of

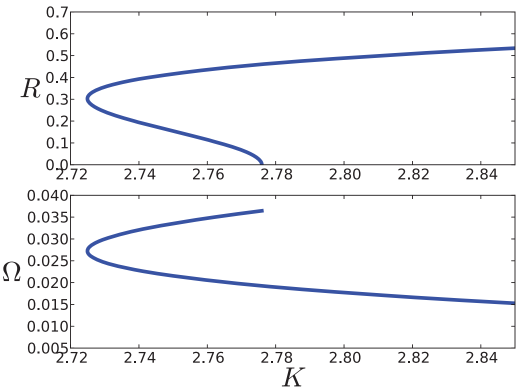

Fig. 4: (Colour on-line) Dependences of R, Ω on the coupling strength K for the correlated distribution (15) with $k = 1$, $D_0 = 1$ and $M_0 = 1.01$.

inertia. We take a distribution

$$G(\omega, M) = \begin{cases} \frac{1}{C}\left(1-\left(\frac{\omega}{D_0}\right)^2\right) & \\ \times\delta(M - M_0 - k\omega), & |\omega| \le D_0, \\ 0, & |\omega| > D_0. \end{cases} \quad (15)$$

where although the partial distribution of frequencies is symmetric, the overall symmetry of $G(\omega, M)$ is broken. In this case, the frequency Ω of the order parameter will be nonzero even for the purely symmetric coupling $\beta = 0$; we illustrate this in fig. 4.

Conclusion. – In conclusion, we have suggested a unified analytic approach that allows to analyze the dynamics of noise-driven populations of globally coupled rotors with a phase shift in the coupling, for arbitrary distribution of their natural frequencies and moments of inertia. In addition to well-studied effects of inertia that lead to a first-order transition to synchrony in the absence of a phase shift in coupling, the method allowed us to study more complex regimes. In the limiting case of vanishing inertia and absence of noise, our model reduces to the Sakaguchi-Kuramoto model of coupled phase oscillators. For the latter, reentrant transition to synchrony [25], in which two ranges of coupling exists for observing synchrony, was observed; we demonstrated a similar phenomenon in our model. Furthermore, the general formulation of our model also includes populations with distributions of moments of inertia of the rotors. A nontrivial effect here is the shift of the frequency of the mean field due to correlations between natural frequencies and the moments of inertia.

* * *

MK thanks the Alexander von Humboldt Foundation for support. SG acknowledges the support of the Indo-French Centre for the Promotion of Advanced Research under Project 4604-3, the warm hospitality of the University of Potsdam, and fruitful discussions with A. Campa and S. Ruffo.

REFERENCES

[1] Kuramoto Y., in *International Symposium on Mathematical Problems in Theoretical Physics, Lecture Notes in Physics*, Vol. **39** (Springer, New York) 1975, pp. 420–422.
[2] Winfree A. T., *J. Theor. Biol.*, **16** (1967) 15.
[3] Kuramoto Y., *Chemical Oscillations, Waves and Turbulence* (Springer, Berlin) 1984.
[4] Acebrón J. A., Bonilla L. L., Vicente C. J. P., Ritort F. and Spigler R., *Rev. Mod. Phys.*, **77** (2005) 137.
[5] Wiesenfeld K., Colet P. and Strogatz S. H., *Phys. Rev. Lett.*, **76** (1996) 404.
[6] Aldridge J. and Pye E. K., *Nature*, **259** (1976) 670.
[7] Michaels D. C., Matyas E. P. and Jalife J., *Circ. Res.*, **61** (1987) 704.
[8] Dörfler F., Chertkov M. and Bullo F., *Proc. Natl. Acad. Sci. U.S.A.*, **110** (2013) 2005.
[9] Néda Z., Nikitin A. and Vicsek T., *Physica A*, **321** (2003) 238.
[10] Inagaki S., *Prog. Theor. Phys.*, **90** (1993) 577.
[11] Antoni M. and Ruffo S., *Phys. Rev. E*, **52** (1995) 2361.
[12] Chavanis P.-H., *Physica A*, **390** (2011) 1546.
[13] Chavanis P. H., *The Brownian mean field model*, arXiv:1306.1203 (2013).
[14] Gupta S., Campa A. and Ruffo S., *Phys. Rev. E*, **89** (2014) 022123.
[15] Sakaguchi H., *Prog. Theor. Phys.*, **79** (1988) 39.
[16] Restrepo J. G. and Meiss J. D., *Onset of synchronization in the disordered Hamiltonian mean field model*, arXiv:1401.3040 (2014).
[17] Sakaguchi H. and Kuramoto Y., *Prog. Theor. Phys.*, **76** (1986) 576.
[18] Tanaka H., Lichtenberg A. and Oishi S., *Phys. Rev. Lett.*, **78** (1997) 2104.
[19] Acebrón J. A. and Spigler R., *Phys. Rev. Lett.*, **81** (1998) 2229.
[20] Acebrón J. A., Bonilla L. L. and Spigler R., *Phys. Rev. E*, **62** (2000) 3437.
[21] Derrida B., Evans M. R., Hakim V. and Pasquier V., *J. Phys. A: Math. Gen.*, **26** (1993) 1493.
[22] Privman V., *Nonequilibrium Statistical Mechanics in One Dimension* (Cambridge University Press, Cambridge) 2005.
[23] Risken H. R., *The Fokker-Planck Equation* (Springer, Berlin) 1989.
[24] Komarov M. and Pikovsky A., *Phys. Rev. Lett.*, **111** (2013) 204101.
[25] Omel'chenko O. E. and Wolfrum M., *Phys. Rev. Lett.*, **109** (2012) 164101.